BIOCHEMISTRY
including biophysical chemistry & molecular biology
Article

Biochemistry **2010,** *49,* 8847–8856 8847
DOI: 10.1021/bi101281f

Transmembrane Helix I and Periplasmic Loop 1 of *Escherichia coli* ProP Are Involved in Osmosensing and Osmoprotectant Transport[†]

Robert A. B. Keates,[‡] Doreen E. Culham,[‡] Yaroslava I. Vernikovska,[§] Adam J. Zuiani,[‡] Joan M. Boggs,[§,∥] and Janet M. Wood*[,‡]

[‡]*Department of Molecular and Cellular Biology, University of Guelph, 488 Gordon Street, Guelph, ON, Canada N1G 2W1,* [§]*Department of Molecular Structure and Function, Research Institute, Hospital for Sick Children, Toronto, ON, Canada M5G 1X8, and* [∥]*Department of Laboratory Medicine and Pathobiology, University of Toronto, Toronto, ON, Canada M5G 1L5*

Received August 10, 2010; Revised Manuscript Received September 9, 2010

ABSTRACT: Osmoregulatory transporters stimulate bacterial growth by mediating osmoprotectant uptake in response to increasing osmotic pressure. The ProP protein of *Escherichia coli* transports proline and other osmoprotectants. Like LacY, ProP is a member of the major facilitator superfamily and a H^+-solute symporter. ProP is regulated by osmotic pressure via a membrane potential-dependent mechanism. A homology model predicts that ionizable and polar residues, highly conserved among ProP homologues, cluster deep within the N-terminal helix bundle of ProP. Chemical labeling of introduced cysteine (Cys) residues supported the homology model by confirming the predicted positions of transmembrane helix I (TMI) and periplasmic loop 1. Replacements of residues in the putative polar cluster impaired or altered ProP function, suggesting that they are important for osmosensing and may interact with the transport substrates. Asn34, Glu37, Phe41, Tyr44, and Ala48 line the most polar face of TMI; Tyr44 is on the periplasmic side of the putative polar cluster, and Ala59 is in periplasmic loop 1. The *N*-ethylmaleimide reactivities of Cys introduced at positions 41, 44, 48, and 59 increased with osmotic pressure, whereas the reactivities of those at cytoplasm-proximal positions 34 and 37 did not. Replacements of polar cluster residues that blocked transport also affected the NEM reactivity of Cys44 and its osmolality dependence. This report and previous work suggest that conformational changes associated with osmosensing may shift the equilibria between outward- and inward-facing transport pathway intermediates.

Increasing osmotic pressure impairs cellular functions, including transport, respiration, and macromolecule synthesis (*1*−*3*). Osmoregulatory transporters forestall these effects and stimulate bacterial growth by mediating the uptake of organic molecules denoted osmoprotectants (*4*−*6*). ProP of *Escherichia coli* transports diverse osmoprotectants, including proline, glycine betaine, and ectoine (*7*). In contrast to the osmotic inhibition of other transporters [e.g., LacY (*3*)], ProP is activated as osmotic pressure increases in cells, in right-side-out membrane vesicles (*8*), and, after purification, in proteoliposomes (*9*). ProP [a member of the major facilitator superfamily (MFS)],[1] BetP of *Corynebacterium glutamicum* [a member of the betaine-choline-carnitine transporter (BCCT) family], and OpuA of *Lactococcus lactis* (a member of the ATP binding cassette transporter family) share this behavior and are denoted osmosensory transporters. They serve as paradigms for the study of osmosensing (*6*).

A homology model is facilitating our efforts to correlate the structural dynamics of ProP with osmoregulation of its activity [Figure 1 (*10*, *11*)]. ProP is related to the three members of the MFS for which crystal structures have been reported: anion antiporter GlpT (*12*), H^+-lactose symporter LacY (*13*), and multidrug resistance transporter EmrD (a H^+-solute antiporter) (*14*). Each crystallized in a cytoplasm-facing conformation, LacY with bound substrate. Our homology model for ProP is based on the crystal structure of GlpT, the closest homologue among the three transporters with known structures (*10*, *11*). The predicted topology and orientation of ProP were substantiated by LacZ−PhoA fusion analysis and fluorescent labeling of cysteine (Cys) residues introduced at the termini and the hydrophilic loops linking putative transmembrane helices of the Cys-less variant ProP* (*10*, *15*). Labeling of introduced Cys also showed that the model correctly predicted the position of TMXII in the membrane (*16*) (Figure 1A). In this paper, we report chemical reactivity data based on a Cys scan of TMI and periplasmic loop 1 (Loop P1). This work

[†]This work was supported in part by an Operating Grant awarded to J.M.W. and J.M.B. (MOP68904) by the Canadian Institutes for Health Research and an Undergraduate Summer Research Award to A.J.Z. from the Natural Sciences and Engineering Research Council of Canada.

*To whom correspondence should be addressed: Department of Molecular and Cellular Biology, University of Guelph, Room 4251 Science Complex, 488 Gordon St., Guelph, ON, N1G 2W1 Canada. Telephone: (519) 824-4120, ext. 53866. Fax: (519) 837-1802. E-mail: jwood@uoguelph.ca.

[1]Abbreviations: $\Delta\mu_{H^+}$, protonmotive force; ΔpH, transmembrane pH gradient, cytoplasm alkaline; ΔΨ, membrane potential, cytoplasm negative; Π, osmotic pressure; Π/RT, osmolality; $\Pi_{1/2}/RT$, osmolality at which the ProP activity is half-maximal; a_0, initial rate of osmoprotectant (proline) uptake via ProP; A_{max}, a_0 at infinite osmolality; *B*, constant inversely proportional to the slope of the curve relating a_0 to Π/RT; BCA, bicinchoninic acid; BCCT, betaine-choline-carnitine transporter; EDTA, ethylenediaminetetraacetic acid; LB, Luria-Bertani; MalPEG, *O*-(2-maleimidoethyl)-*O*′-methyl-poly(ethylene glycol) 5000; MFS, major facilitator superfamily; MOPS, 4-morpholinopropanesulfonic acid; MTS, methanethiosulfonate; MTSEA, (2-aminoethyl)methanethiosulfonate; MTSES, (2-sulfonatoethyl)methanethiosulfonate; MTSET, [2-(trimethylammonium)ethyl]methanethiosulfonate; MW, molecular weight; NEM, *N*-ethylmaleimide; NAO, 10-*N*-nonyl-3,6-bis(dimethylamino)acridine; OD, optical density; ORF, open reading frame; OGM, Oregon Green Maleimide; PCR, polymerase chain reaction; PDB, Protein Data Bank; PE, phosphatidylethanolamine; PG, phosphatidylglycerol; PMSF, phenylmethanesulfonyl fluoride; PRL, proteoliposome; SDS−PAGE, sodium dodecyl sulfate−polyacrylamide gel electrophoresis; TM, transmembrane; WT, wild type.

Published on Web 09/09/2010

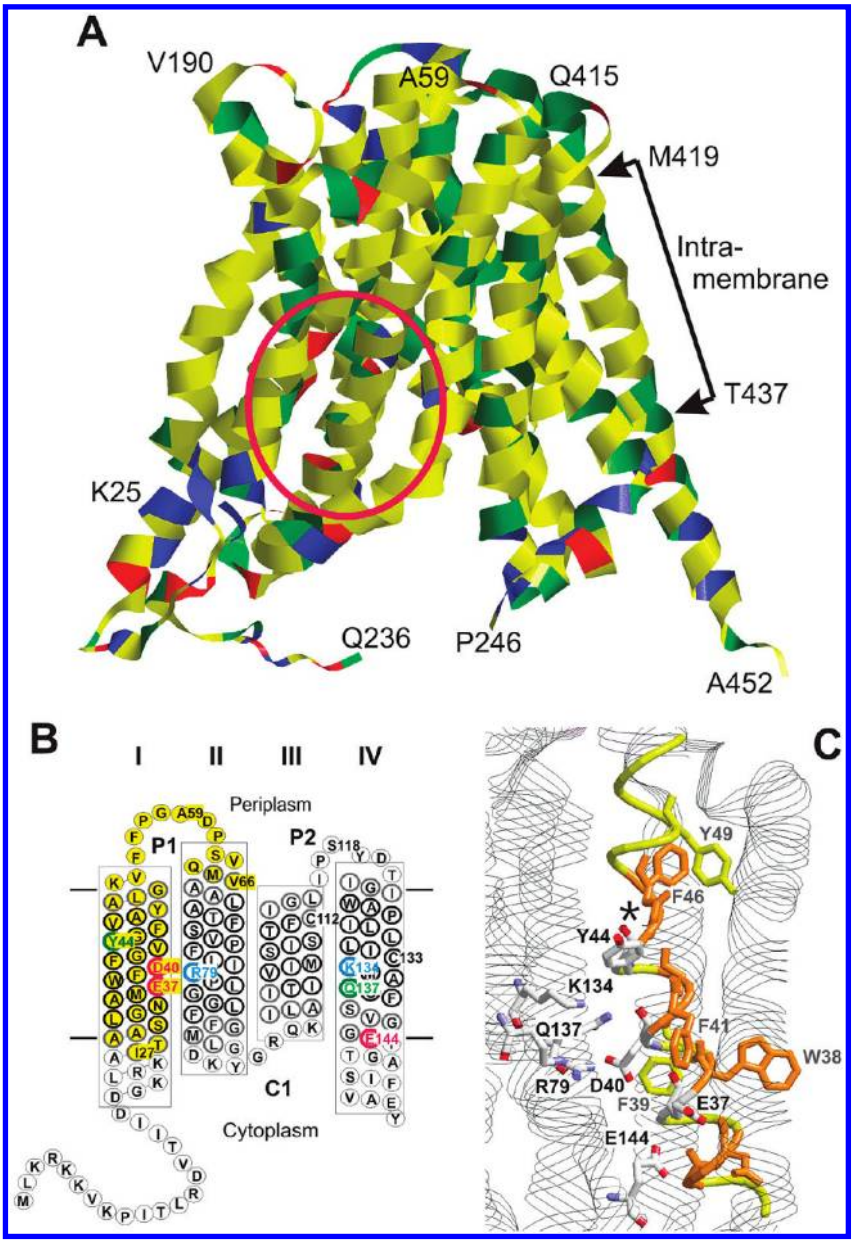

FIGURE 1: Structural representations of ProP. (A) Homology model for ProP (*10*, *11*). Colors designate residues that are nonpolar (yellow), polar (green), acidic (red), or basic (blue). The experimentally determined limits of TMXII [M419−T437 (*16*)] are marked with arrows. The red circle encloses residues also shown in panels B and C. (B) Membrane topology of residues M1−Y155 of ProP substantiated by protein fusion- and chemical labeling-based analyses (*10*, *11*, *15*, *16*). Boxes enclose putative helices. Bold gray and black circles indicate interfacial and intramembrane residues, respectively. Yellow highlighting indicates native Cys and residues converted to Cys in the background of ProP* [Cys-less ProP-His_6 (*15*)] for this study. Conserved, polar residues predicted to cluster within the N-terminal helix bundle (*10*, *11*) are circled in A, highlighted in B (red for acidic, blue for basic, and green for polar), and labeled in C. (C) N-Terminal helix bundle, with intramembrane TMI residues 31−52 shown as a yellow and orange trace. Conserved, polar residues E37, D40, Y44, R79, K134, Q137, and E144 are implicated in osmosensing and transport (Figures 5, 6, and 8) (*10*, *11*). ProP activity is also dramatically reduced when residues colored orange (G33, N34, W38, F41, and G42) are replaced with Cys (Figure 2). The asterisk marks a predicted kink in TMI.

supports the predicted position of TMI and provides insights into the structure of Loop P1.

As a H^+-solute symporter, ProP may function via an alternating access mechanism analogous to that of well-characterized MFS member LacY (*17*). Like LacY, ProP is powered by the protonmotive force ($\Delta\mu_{H^+}$) that is comprised of a pH gradient (ΔpH, alkaline inside the cell) and a membrane potential (ΔΨ, negative inside) (*7*, *8*, *18*). In addition, ΔΨ controls osmosensing by ProP (*3*). ProP activity is extremely low and osmolality-independent in proteoliposomes without ΔΨ, even if ΔpH is present. ProP activity remains osmolality-independent at low ΔΨ values (e.g., −100 mV), but it responds as a sigmoid function of the osmolality as ΔΨ approaches that of actively respiring *E. coli* (−137 mV). Thus, at high ΔΨ values (e.g., −120 to −137 mV), ProP activity is suppressed at low osmolality (high water activity) (*3*). The osmolality and ΔΨ may affect ProP activity by shifting the equilibria between intermediates along the transport pathway.

Polar and ionizable residues cluster within the membrane in the C-terminal helix bundle, not in the N-terminal helix bundle, of LacY. These residues are implicated in β-galactoside transport (*17*). In contrast, no polar or ionizable residues are predicted to occur within the membrane in the C-terminal bundle of ProP.

Our homology model predicts that highly conserved polar residues E37, D40, Y44, R79, K134, Q137, and E144 form a contiguous cluster, deep in the membrane, in the N-terminal helix bundle of ProP (Figure 1A−C). That prediction is supported by our data confirming the position of TMI. Here we also show, via amino acid replacements, that the conserved polar residues within TMI, TMII, and TMIV are important for ProP function.

Structural dynamics associated with osmosensing can be monitored by detecting changes in the reactivities of introduced Cys residues that reflect changes in their environments. Previously, we reported effects of the osmolality and $\Delta\mu_{H^+}$ on the *N*-ethylmaleimide (NEM) reactivities of Cys residues introduced into periplasmic loops of ProP (*11*). Cys thiols in Loops P1 and P6 (Cys59 and Cys415) increased in reactivity with increasing osmolality much more than Cys thiols in Loops P2−P5. However, the reactivity of Cys59 did not increase with osmolality if $\Delta\mu_{H^+}$ was collapsed with a proton ionophore [carbonyl cyanide *m*-chorophenylhydrazone (CCCP)] or if a mutation that makes ProP activity osmolality-insensitive was introduced. Here we report the effect of osmolality on the NEM reactivities of residues lining one face of TMI. These data show that the conformational change associated with osmosensing extends deep into the membrane toward the polar cluster associated with transport but does not alter the reactivities of cytoplasm-proximal residues. In addition, replacement of residues in the putative polar cluster altered the osmolality-dependent NEM reactivity of Cys44, underscoring the importance of these residues for both osmosensing and transport.

EXPERIMENTAL PROCEDURES

Materials and Culture Media. Oligonucleotides were purchased from Cortec DNA Services (Kingston, ON) or Eurofins MWG Operon (Huntsville, AL). Bovine pancreatic DNase I (type II) was from Boehringer-Mannheim (Laval, QC) and Sigma-Aldrich (Oakville, ON). Egg white lysozyme (UltraPure grade) was from Caledon Laboratories (Georgetown, ON) and Sigma-Aldrich (Oakville, ON). Oregon Green 488 Maleimide carboxylic acid (OGM) was from Molecular Probes Inc. (Eugene, OR). 2-(Aminoethyl)methanethiosulfonate (MTSEA), 2-(sulfonatoethyl)methanethiosulfonate (MTSES), and methanethiosulfonate ethyltrimethylammonium (MTSET) were from Toronto Research Chemicals Inc. (Toronto, ON). OGM, MTSEA, MTSES, and MTSET were prepared as stock solutions in *N*,*N*-dimethylformamide (Fisher Scientific Inc., Nepean, ON) and stored at −20 °C, protected from light, prior to use. *O*-(2-Maleimidoethyl)-*O*′-methylpoly(ethylene glycol) 5000 (MalPEG) was from Sigma-Aldrich (catalog no. 63187). Carbonyl cyanide *m*-chlorophenylhydrazone (CCCP), *N*-ethylmaleimide (NEM), ampicillin, imidazole, and β-mercaptoethanol were from Sigma Chemical Co. (St. Louis, MO). NEM was prepared as a stock solution in ethanol. Horseradish peroxidase (HRP)-conjugated anti-PentaHis antibody and Ni-NTA resin were from Qiagen, Inc. (Mississauga, ON). Other reagents were of the highest grade available. Solution osmolalities were measured with a Wescor (Logan, UT) vapor pressure osmometer.

Bacteria were cultivated at 37 °C in LB medium (*19*) or in NaCl-free MOPS medium, a variant of the MOPS medium described by Neidhardt et al. (*20*) from which all NaCl had been omitted. This base medium was supplemented with NH_4Cl (9.5 mM) as a nitrogen source and glycerol [0.4% (v/v)] as a carbon source. L-Tryptophan (245 μM) and thiamine hydrocholoride (1 μg/mL) were added to meet auxotrophic requirements, creating a complete growth medium with an osmolality of 0.14−0.15 mol/kg. Ampicillin (100 μg/mL) was added as required to maintain plasmids. Arabinose was added as specified to ensure that all ProP variants were expressed at similar levels.

Bacteria, Plasmids, and Molecular Biological Manipulations. Basic molecular biological techniques were as described by Sambrook et al. (*21*). Both *proP* expression and ProP activity are osmoregulated (*22*). To focus on the osmoregulation of transporter activity in vivo, genes encoding ProP variants were expressed at a physiological level and in an osmolality-independent manner from the AraC-controlled P_{BAD} promoter of plasmid pBAD24 (*23*). ProP variants were expressed in plasmid-bearing derivatives of *E. coli* WG350 [F^- *trp lacZ rpsL thi* Δ(*putPA*)*101* Δ(*proU*)*600* Δ(*proP-melAB*)*212*] (*24*). Each strain contained plasmid pDC79 [a derivative of pBAD24 encoding wild-type ProP (*25*)], pDC117 [a derivative of pBAD24 encoding the fully functional Cys-less variant of ProP-His_6 with amino acid replacements C112A, C133A, C264V, and C367A, denoted ProP* (*15*)], or a derivative of one of those plasmids. Plasmids encoding these variants were created by site-directed mutagenesis as previously described (*15*).

Transport Assays. Published procedures were used to cultivate bacteria in NaCl-free MOPS medium and to measure proline uptake (*26*). The expression levels of ProP variants were determined by conducting Western blots on whole cell extracts using anti-PentaHis antibodies for ProP* and its variants or anti-ProP antibodies for ProP and its variants, as previously described (*25*). Transport assay media were adjusted to the indicated osmolalities with NaCl or sucrose. For the data reported in Figures 2B,C and 5A,B, initial rates of proline uptake at low and high osmolality (a_L and a_H, respectively) were measured in media supplemented with 50 and 170 mM NaCl to produce osmolalities of 0.24 and 0.49 mol/kg, respectively. All transport measurements were performed in triplicate on at least two separate days. Unless otherwise stated, figures show representative means and standard errors of the mean for triplicate assays performed on one day. The osmotic activation ratio was calculated as a_L/a_H. Where indicated, the initial rate of proline uptake (a_0) attained at a particular medium osmolality (Π/RT) was fit to eq 1:

$$a_0 = A_{max}\{1 + \exp[-(\Pi - \Pi_{1/2})/(RTB)]\}^{-1} \quad (1)$$

where A_{max} is the uptake rate that would be observed at infinite osmolality, R is the gas constant, T is the temperature, $\Pi_{1/2}/RT$ is the medium osmolality yielding half-maximal activity, and B is a constant inversely proportional to the slope of the response curve.

Site-Directed OGM Labeling. As previously described (*10*, *15*, *16*), the reactivities of Cys residues in ProP* variants were determined by OGM (40 μM) labeling of permeabilized membranes. Cys-less ProP* was included to determine background labeling. For certain variants that were not labeled well with OGM, permeabilized membranes were pretreated with MTS reagents (0.2 mM) and then the proteins were labeled with OGM in SDS to determine their reactivities with reagents with varying charges (*10*). For these experiments, bacteria were cultivated in LB medium (*19*) and expression of ProP* or its variant was induced via addition of L-arabinose (1.66 mM) 1 h before the culture was harvested. OGM labeling and protein recovery were estimated by densitometry of SDS−PAGE gels of the purified ProP* variants. The OGM reactivity of each protein was estimated as the ratio of the density of the fluorescent band to that of the Coomassie Blue-stained band with the electrophoretic

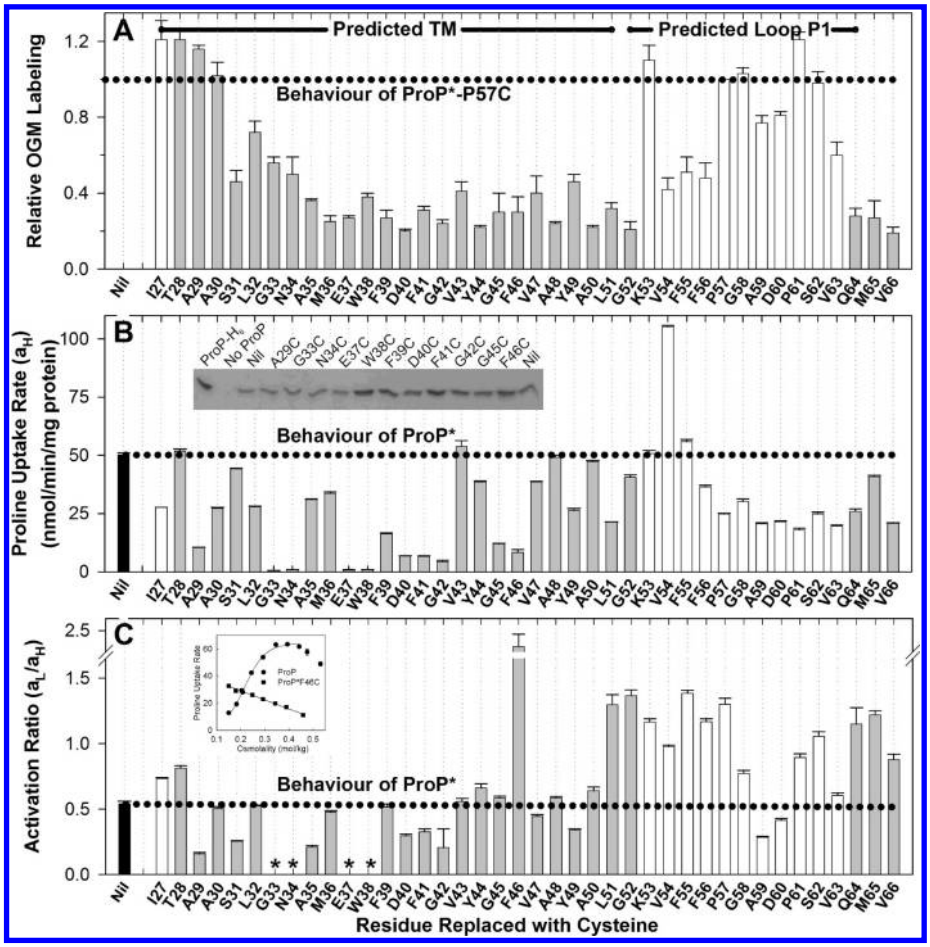

FIGURE 2: Structure−function analysis of cysteines introduced into ProP*. Structural (A) and functional (B and C) assays were performed on membranes or bacteria containing ProP* variants in which Cys replaced residues I27−V66. Each residue was predicted to form part of a TM (I or II, gray) or Loop P1 (white) (see Figure 1A). Bacteria were cultivated as described in Experimental Procedures, and arabinose (1 μM) was included to increase the expression level of variant ProP*F39C. On each horizontal axis, Nil represents ProP*. (A) OGM labeling of Cys in membranes indicates its accessibility in an aqueous environment. ProP* variants in permeabilized membrane preparations were labeled with OGM, purified, and analyzed by SDS−PAGE as described in Experimental Procedures. The figure represents the proportion of the recovered protein that was labeled with the OGM fluor. ProP*P57C was arbitrarily selected as the normalization standard. (B and C) The proline uptake activities (nanomoles per minute per milligram) of cells expressing the ProP* variants were measured at low and high osmolalities [0.24 mol/kg (a_L) and 0.49 mol/kg (a_H), respectively] as described in Experimental Procedures. In panel B, a_H estimates the maximum transporter activity. In panel C, a_L/a_H (the activation ratio) estimates the dependence of activity on osmolality. a_L/a_H is 0.52 for ProP*, lower for variants that activate at higher osmolalities, and higher for osmolality-insensitive variants. Asterisks indicate that activities were too low for the reliable estimation of ratios. In the inset of panel B, variants were expressed at similar levels as determined by Western blotting. Representative Western blot data are shown. The lane labeled ProP-His$_6$ was loaded with 15 ng of the purified protein. The inset of panel C shows an expanded view of the dependence of the activity of variant ProP*F46C on osmolality.

mobility of ProP, normalized to the corresponding ratio for ProP*_P57C. Each experiment was performed twice. The ratios from two different experiments were averaged to give the mean ± range reported in Figures 2A and 3.

Site-Directed PEGylation. The reactivities of Cys residues were also assessed by blocking with NEM and back-labeling with MalPEG (*27*). ProP variants were cultivated in 24 mL of NaCl-free MOPS medium as previously described for transport assays (*26*). Cells were collected by centrifugation at 3420*g* for 10 min and resuspended in 24 mL of unsupplemented MOPS medium (*26*) to which 11 mM glucose and 35 mM NaCl had been added (osmolality of 0.15 mol/kg). Cell suspensions were divided into 12 mL aliquots. One aliquot received 12 μL of 50 mM NEM in absolute ethanol, and the other received 12 μL of absolute ethanol only. The resulting mixtures were incubated at 25 °C for 20 min in a shaking water bath. Cells were then collected by centrifugation as described above, washed in glucose-free medium, and re-collected. Membranes were prepared by suspending each cell pellet in 2 mL of lysis buffer [10 mM Tris-HCl, 5 mM EDTA, 300 μg/mL lysozyme, 40 μg/mL DNase I, and 1 mM phenylmethanesulfonyl fluoride (PMSF) (pH 7.5)], incubating each at room temperature for 15 min, and diluting each into 18 mL of ice-cold water. Membranes were collected by centrifugation at 31000*g* for 20 min, washed in water, centrifuged again, and solubilized by repetitive pipeting in solubilization buffer [0.5 mL of 20 mM potassium phosphate, 2 mM EDTA, 140 mM NaCl, and 1% (w/v) SDS (pH 8.0)]. Unreacted Cys residues were detected via addition of MalPEG (25 μL) to a final concentration of 0.64 mM. Samples were incubated for 15 min at 4 °C for ProP* variants with Cys at positions 51, 53, 54, 55, 56, or 57 and for 30 min at 37 °C for all other variants. PEGylation was terminated via addition of 130 μL of 5-fold concentrated SDS−PAGE sample buffer [0.3 M Tris, 10% (w/v) SDS, 50% (v/v) glycerol, 0.125% (w/v) bromophenol blue, and 25% (v/v) 2-mercaptoethanol (pH 6.8)]. This procedure was performed three times, and the proportion of ProP molecules with reduced electrophoretic moblility

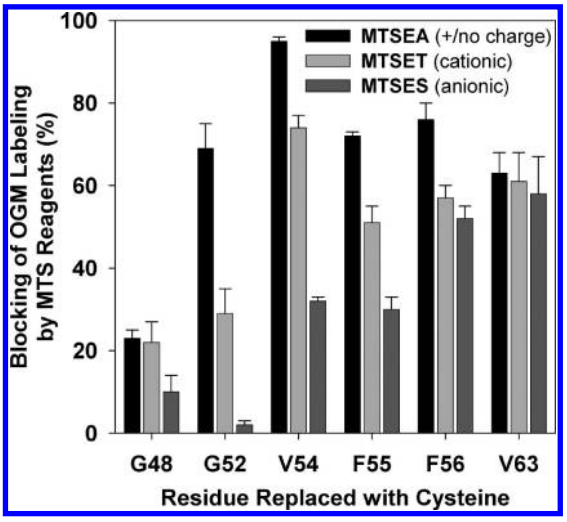

FIGURE 3: MTS reagents differentially block OGM labeling of Cys introduced into ProP*. The Cys reactivities were assessed by OGM labeling of SDS-solubilized ProP* variants, without or with prior treatment of permeabilized membranes with MTS reagents, as described in Experimental Procedures.

due to PEGylation was determined by Western blotting and densitometry. Western blotting was performed as described previously (*25*) except that the iBlot Dry Blotting System was employed with nitrocellulose membrane gel transfer "stacks" (Invitrogen Corp.). Alternative systems produced much more efficient transfer of the PEGylated proteins than of the unPEGylated proteins.

The procedure described above was modified as follows to determine how $\Delta\mu_{H^+}$ and the osmolality affected the reactivities of cysteines with NEM. Cells were cultivated in 100 mL of NaCl-free MOPS medium (*26*); cultures were divided into four 24 mL aliquots, and cells were collected by centrifugation at 3420*g* for 10 min and resuspended in 24 mL of MOPS medium supplemented with either 11 mM glucose or 10 μM CCCP, with and without the addition of 150 mM NaCl to adjust the osmolality. NEM was added to a final concentration of 50 or 100 μM, and samples were then treated as described above.

RESULTS

Membrane Insertion of TMI and Limits of Periplasmic Loop 1. Our homology model places TMI between T28 and G52 and TMII between Q64 and M88. We used chemical labeling of introduced Cys residues to determine the positions of TMI and the periplasmic end of TMII within the membrane, thereby also defining the limits of Loop P1. These experiments exploit the fact that maleimides and methanethiosulfonates react with exposed Cys thiols in polar (but not nonpolar) environments. In preparation for this analysis, residues 27−66 of Cys-less ProP variant ProP* were replaced with Cys and the expression and function of the resulting variants were characterized. Some variants were inactive (Figure 2B, discussed further below), and some Cys replacements altered the osmolality response as indicated by the osmotic activation ratio (Figure 2C). Low and high ratios usually indicate elevation and lowering of the osmolality required to activate ProP, respectively (*10*, *15*). ProP*F46C was unusual in that its activity decreased steadily with increasing osmolality (inset of Figure 2*C*). This behavior is characteristic of LacY (*3*) and other transporters that do not contribute to osmoregulatory solute accumulation. The variants were expressed at similar levels as indicated by Western blotting (see the inset of Figure 2B).

Labeling with OGM, a bulky, membrane-impermeant maleimide, was used to determine the limits of TMI and Loop P1. Permeabilized membranes from bacteria grown in arabinose (1.66 mM)-supplemented LB medium were treated with OGM at a low osmolality. Thus, ProP levels were elevated slightly; $\Delta\mu_{H^+}$ was absent, and ProP was not osmotically activated. OGM did not react well with Cys at positions 31−52 or 64−66 (Figure 2A), suggesting that the buried portion of TMI extends from approximately S31 to G52, residues K53−V63 constitute Loop P1, and residues Q64−V66 are near the periplasmic end of TMII. Thus, the residues at positions 28−30 are more exposed to the cytoplasm than predicted by our model (prediction indicated by the gray bars in Figure 2A).

The Cys residues at positions 54−56 were less reactive than expected for residues in a fully exposed loop. We therefore investigated the abilities of thiol-reactive MTS reagents with various charges to block subsequent OGM labeling of Cys at these positions in the SDS-solubilized protein. MTSEA exists in uncharged and cationic forms at physiological pH, whereas MTSET and MTSES are cationic and anionic, respectively. OGM labeling of Cys at positions 52, 54−56, and 63 could be blocked by prior treatment of cells with one or more of these reagents, whereas the limited OGM labeling of C48 was affected very little by such treatment (Figure 3). MTSEA and MTSET were more effective at most sites than MTSES, suggesting that residues 54−56 are in Loop P1 but not accessible to anionic OGM or MTSES. The reactivity of C52 with MTSEA suggests that Loop P1 begins with residue 52.

The exposure of residues in Loop P1 was also assessed by NEM blocking of intact cells followed by MalPEG labeling of the SDS-solubilized protein (Figure 4). In this case, intact, energized cells expressing the ProP variants at a physiological level were treated with membrane-permeant, uncharged NEM under conditions similar to those used for transport assays at low osmolalities. The 5 kDa poly(ethylene glycol) moiety of MalPEG reduced the electrophoretic mobility of the target protein so that labeled (PEGylated) and unlabeled proteins could be imaged simultaneously (Figure 4A). Completion of this analysis before and after NEM alkylation yielded estimates of NEM reactivity (Figure 4B). NEM did not block PEGylation of Cys at position 50, 51, or 66, suggesting that they define the periplasmic ends of TMs I and II. NEM strongly blocked PEGylation of the variants with Cys residues at positions 52−65 (Figure 4B), so Cys residues at those positions are NEM-accessible and solvent-exposed. Incomplete PEGylation was observed for the unblocked, SDS-solubilized ProP* variants with Cys residues at positions 58−63. Access to these Cys residues by the bulky MalPEG reagent may be blocked by residual secondary structure, even in SDS. The data reported in Figures 2−4 suggest that PEGylation can be used as an alternative to other labeling techniques for the assessment of Cys reactivity.

Functional Significance of the Putative Polar Cluster. The data discussed above indicate that E37 and D40 are buried deep within the membrane where they may cluster with residues R79, K134, Q137, and E144 (Figure 1C). ProP activity was significantly impaired when each of these residues was replaced, in turn, with an isosteric, nonpolar residue. In some cases, conservative replacements also impaired activity (D versus E or K versus R) (Figure 5A). Thus, some residues appeared to be essential (E37, R79, and E144), whereas others were not (D40, K134, and Q137). Conservative replacements R79K and E144D eliminated activity, whereas a trace of activity remained when residue E37 was

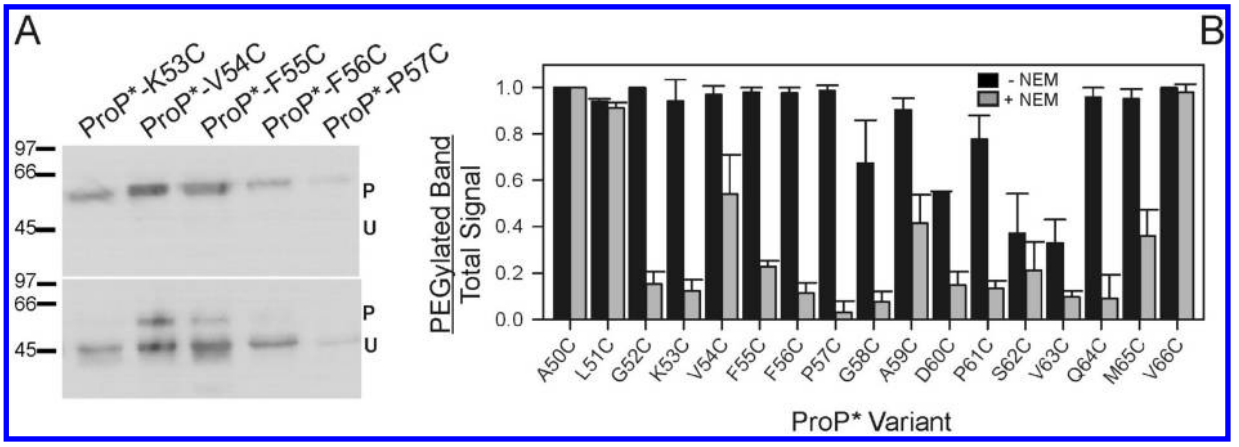

FIGURE 4: NEM differentially blocks PEGylation of Cys residues introduced into ProP*. The reactivities of Cys residues introduced into ProP* were assessed by PEGylating SDS-solubilized ProP* variants obtained from bacteria that were or were not pretreated with NEM (50 μM) as described in Experimental Procedures. (A) The His tag of ProP* was detected by Western blotting to reveal both PEGylated (P) and unPEGylated (U) ProP* variants. Samples were from bacteria that were not (top) or were (bottom) treated with NEM. (B) This procedure was repeated with three bacterial cultures expressing each ProP* variant. Densitometry was performed using ImageJ. The graph depicts the fractions of total signal corresponding to the PEGylated protein in samples from untreated and NEM-treated bacteria (black and gray bars, respectively, each representing the mean ± standard deviation for three replicates). Some residues remained refractory to labeling in SDS (e.g., C63).

replaced with D. Some replacements affected the sensitivity of the transporter to osmotic stress as indicated by the activation ratio, a_L/a_H (Figure 5B). Titrations showed that replacements D40E, D40V, Q137N, and K134L lowered the osmolality at which ProP became active (Figure 5C,D) as well as the amplitude of that activation (Figure 5A and figure legend), but they did not block transport. These results reinforced evidence, obtained by Cys scanning, that residues in TMI are critical for ProP function (Figure 2B,C). Replacement of G33, N34, E37, W38, D40, F41, or G42 with Cys dramatically impaired ProP activity, and all those residues are predicted to cluster within the N-terminal helix bundle, just below a kink in TMI (Figure 1C).

Y44 is predicted to cap the cluster of intramembrane polar residues on its periplasmic side (Figure 1C). We previously reported that replacement Y44M renders ProP osmolality-insensitive (*11*). Replacement of Y44 with F had little effect on ProP function, whereas the effects of S and C replacements were intermediate (Figure 6A). These results suggested that the aromatic ring at position 44 is important for the osmolality response. However, further analysis, reported below, qualified that conclusion.

The Osmolality Alters the NEM Reactivities of Periplasm-Proximal TMI Residues. We previously showed that the NEM reactivity of C59 (Loop P1) increased with the osmolality (*11*). These measurements were extended to determine whether the conformational changes affecting C59 reactivity extend into the membrane core.

Variant ProP*Y44C was selected for initial study because of the capping position of Y44. In addition, in contrast to the behavior of ProP_Y44C, the absolute activity and osmolality dependence of ProP*Y44C are very similar to those of ProP* and wild-type ProP (Figures 2B,C and 6B). Like ProP*A59C, ProP*Y44C was more NEM-reactive at high than at low osmolality (Figure 7B). In Figure 7, gray bars, representing the proportion of ProP PEGylated after NEM treatment of intact bacteria, are superimposed on black bars, representing the proportion of ProP PEGylated without prior NEM treatment.

We extended this study by comparing the NEM reactivity of ProP*A59C with the reactivities of variants in which Cys replaced A48, Y44, F41, E37, or N34 (Figure 7). The latter residues line the most polar face of TMI (Figure 7A). Variants ProP*59C, -48C, and -44C retain osmoregulated transport activity (Figure 2B). Mutation A59C elevates the osmolality at which ProP becomes active, but ProP*59C is activated at the "high" osmolality used for these experiments (*11*). Variants ProP*41C, -37C, and -34C have little or no activity (Figure 2B). They were included in this analysis because, as shown below, a mutation impairing transport did not block the osmotically induced change in the NEM reactivity of C44.

The PEGylation assay revealed that the osmotically induced increase in NEM reactivity extended from Loop P1 (residue 59C) into the membrane core to also affect residue 41C but not residue 37C or 34C (Figure 7B). Thus, an osmotically induced conformational change increased the level of exposure of some residues in the periplasmic half of TMI to a polar environment.

Impact of Transport-Blocking Mutations on the NEM Reactivity of C44. We probed the relationship between osmosensing and transport by determining the impacts of mutations E37D, R79K, and E144D on the NEM reactivity of C44. Each mutation abrogated the activities of wild-type ProP (Figure 5A) and variant ProP*Y44C (data not shown). Interestingly, each mutation had a different effect on the osmolality-dependent reactivity of C44. ProP*E37D_C44 was more NEM-reactive at high than at low osmolality, mirroring the osmolality-dependent reactivity of C44 in ProP*. ProP*Y44C_R79K and ProP*Y44C_E144D displayed markedly different behavior, although slight increases in NEM reactivity at high osmolality were observed. Mutation E144D essentially blocked, while R79K enhanced, the NEM reactivity of C44 at low osmolality. The former mutation may favor an inactive transporter conformation and the latter an active conformation. Mutation R79K had no significant effect on the NEM reactivity of C44 at high osmolality, while E144D decreased that reactivity. Again, E144D appeared to favor an inactive transporter conformation.

Impact of $\Delta\mu_{H^+}$ on the NEM Reactivities of Residues in TMI and Periplasmic Loop 1. We previously reported that the osmotically induced increase in NEM reactivity of C59 (Loop P1) occurred in glucose-energized but not in CCCP-treated bacteria (which maintain and lack $\Delta\mu_{H^+}$, respectively) (*11*). In this work, small decreases in NEM reactivity were consistently observed when CCCP replaced glucose at high osmolalities (Figures 7C and 8).

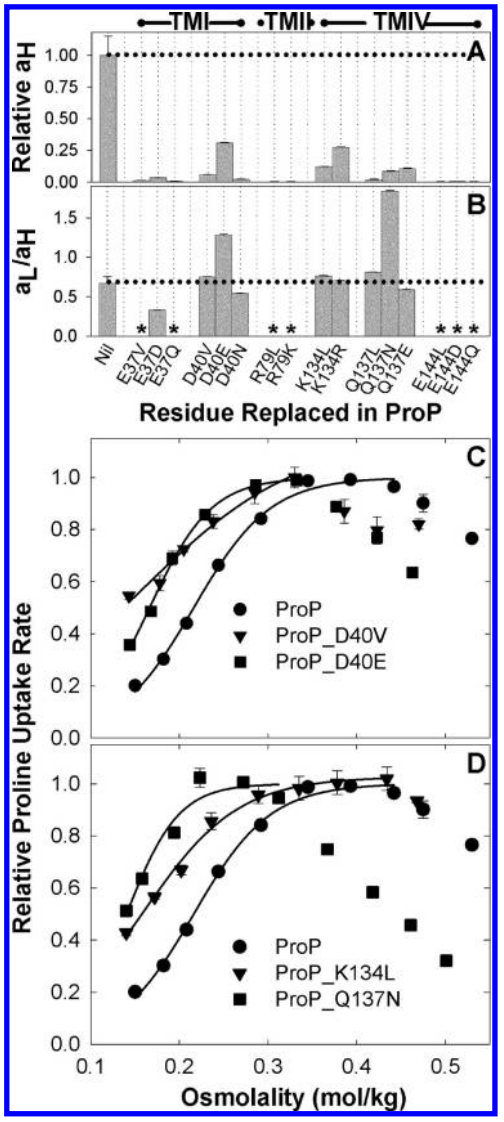

FIGURE 5: Impact of replacements of intramembrane polar or charged ProP residues. Residues E37 and D40 (TMI), R79 (TMII), and K134, Q137, and E144 (TMIV) of wild-type ProP were replaced with isosteric nonpolar residues or homologues. Each variant was expressed from plasmid pBAD24 in *E. coli* WG350, which lacks proline uptake activity (see Experimental Procedures). With the exception of ProP_E37V, the variants were expressed at levels comparable to that of wild-type ProP as determined by Western blotting (data not shown). Bacteria expressing ProP_E37V were cultivated with 28 μM arabinose to increase its level of expression to the same level. The proline uptake activities of the variants were determined at low (a_L, 0.24 mol/kg) and high (a_H, 0.49 mol/kg) osmolalities, or at a series of osmolalities, as described in Experimental Procedures. (A) The activities at high osmolality (a_H) are expressed relative to that of wild-type ProP, which was 68 $\pm$ 10 nmol min^{-1} (mg of protei)$^{-1}$ (mean and standard error determined in triplicate assays in nine independent experiments). (B) The osmotic activation ratios (a_L/a_H) are compared with that of wild-type ProP [0.67 $\pm$ 0.08 (mean and standard error determined with triplicate assays in nine independent experiments)]. Asterisks designate values that could not be calculated with certainty because the corresponding a_L and a_H values were too low. (C and D) The proline uptake activities of the variants were determined at the indicated osmolalities as described in Experimental Procedures and are shown as relative rates to highlight the curve shapes. Data were fit to eq 1; regression lines are plotted, and activities are expressed relative to A_{max} (see Experimental Procedures). The A_{max} values of the variants (in nanomoles per minute per milligram of protein) were 4.5 $\pm$ 0.6 for ProP_D40V, 33.6 $\pm$ 0.6 for ProP_D40E, 13.0 $\pm$ 0.3 for ProP_K134L, and 14.8 $\pm$ 0.4 for ProP_Q137N.

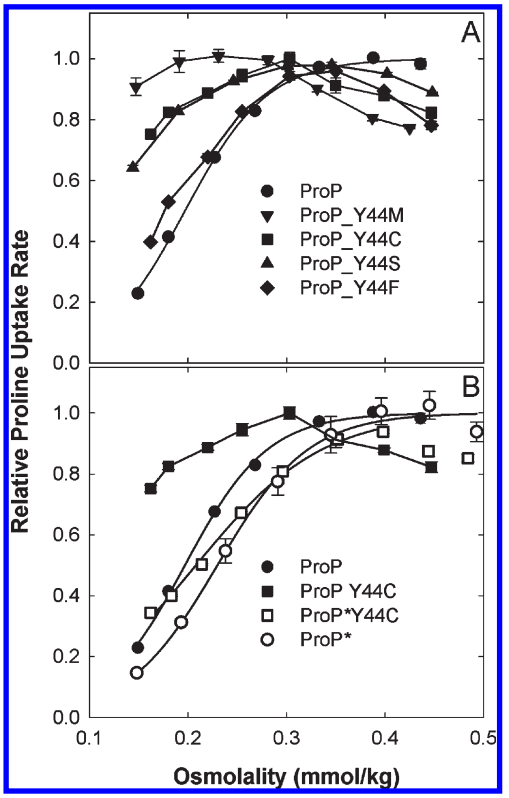

FIGURE 6: Impact of replacements of Y44 on ProP function. Residue Y44 of wild-type ProP or Cys-less, histidine-tagged ProP (ProP*) was replaced with M, F, C, or S as described in Experimental Procedures. Each variant was expressed from plasmid pBAD24 in *E. coli* WG350, which lacks proline uptake activity (see Experimental Procedures). Bacteria were cultivated as described in Experimental Procedures. Arabinose (15 μM) was added to elevate the level of expression of variant ProP_Y44S, and each variant was expressed at a level comparable to that of wild-type ProP as determined by Western blotting (data not shown). The proline uptake activities of the variants were determined at the indicated osmolalities as described in Experimental Procedures and are shown as relative rates to highlight the curve shapes. Activities are expressed relative to the maximal values for ProP_Y44M, ProP_Y44C, ProP_Y44S, and ProP_Y44F. For the other variants, data were fit to eq 1, regression lines are plotted, and activities are expressed relative to A_{max} (see Experimental Procedures). The values used for normalization were as follows (in nanomoles per minute per milligram of protein): 63.9 $\pm$ 0.7 for ProP, 28.7 $\pm$ 0.8 for ProP_Y44M, 48.7 $\pm$ 1.0 for ProP_Y44C, 37.9 $\pm$ 0.3 for ProP_Y44S, 48.2 $\pm$ 0.9 for ProP_Y44F, and 33.4 $\pm$ 0.5 for ProP*Y44C.

However, this decrease was statistically significant in only two cases [variant ProP*Y44C (treated with 50 μM NEM) (Figure 7B) and variant ProP*Y44C_R79K (treated with 100 μM NEM) (Figure 8)].

DISCUSSION

Limits of TMI and TMII. The homology modeling of ProP was contingent on identification of the ProP residues that form TM helices, and the predicted position of TMI was least certain. Uncertainty arose in part because polar residues E37 and D40 were predicted to be in the middle of TMI and a run of apolar residues extending into Loop P1 allowed for a possible alternative placement of TMI. The reactivities of introduced Cys residues with OGM, MTS reagents, and NEM were therefore examined to determine the position of TMI (Figures 2A, 3, and 4, respectively).

The limited OGM reactivities of C37 and C40 (Figure 2A) confirm that residues E37 and D40 are deep within the buried portion of TMI. Residues C28, C29, and C30 are labeled by OGM

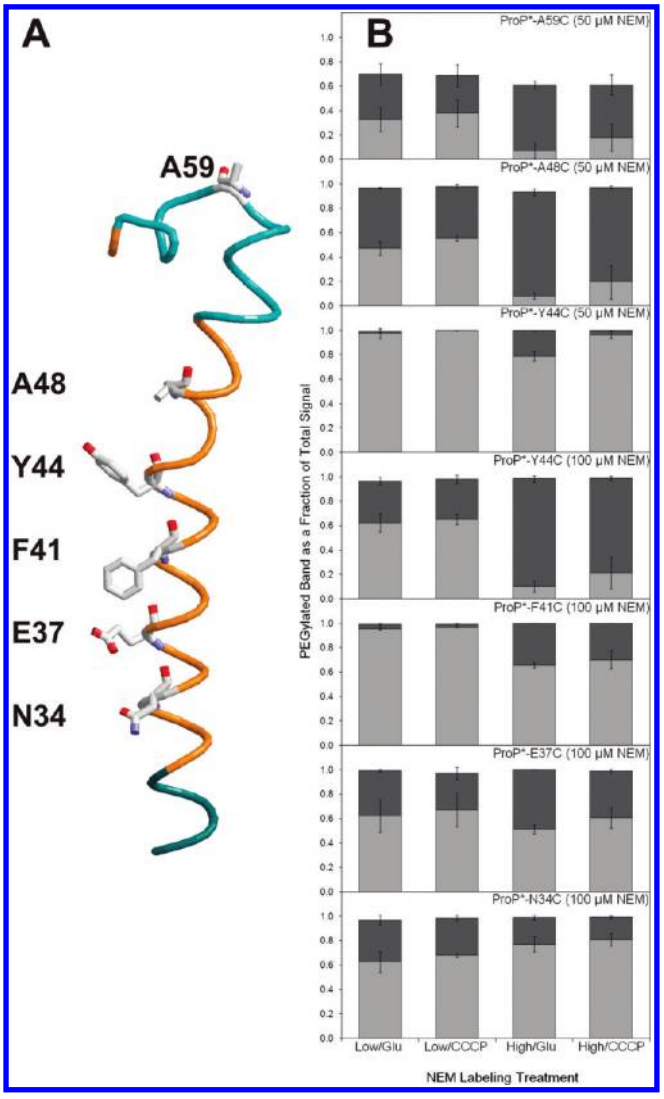

FIGURE 7: Impacts of $\Delta\mu_{H^+}$ and osmolality on the NEM reactivities of Cys residues introduced into TMI. (A) Structure of TMI and Loop P1 according to our structural model (Figure 1) and experimental data. The backbone corresponding to residues in TMI or TMII is colored gold, and that in Loop P1 is colored aqua. (B) Bacteria expressing ProP* derivatives with a Cys introduced at position 34, 37, 41, 44, 48, or 59 were (overlying gray bars) or were not (underlying black bars) treated with NEM in medium supplemented with glucose or CCCP and at low (0.15 mol/kg) or high (0.43 mol/kg) osmolality before solubilization and labeling with MalPEG, as described in the legend of Figure 4. The replaced residues are highlighted in panel A (side chains shown and labeled). The difference in height between the gray and black bars represents the extent to which reaction with NEM blocks reaction of each Cys with MalPEG. The NEM concentration (50 or 100 μM) was selected to reveal the effects of the osmolality and facilitate comparisons among residues. The proportions of PEGylated and unPEGylated ProP were determined by Western blotting, as described, for three independent experiments, and error bars represent standard deviations of the means. Independent experiments showed that the initial rate of proline uptake by Cys-less variant ProP* was reduced 18 and 27% by treatment with 50 and 100 μM NEM, respectively, under conditions similar to those used for this NEM reactivity study.

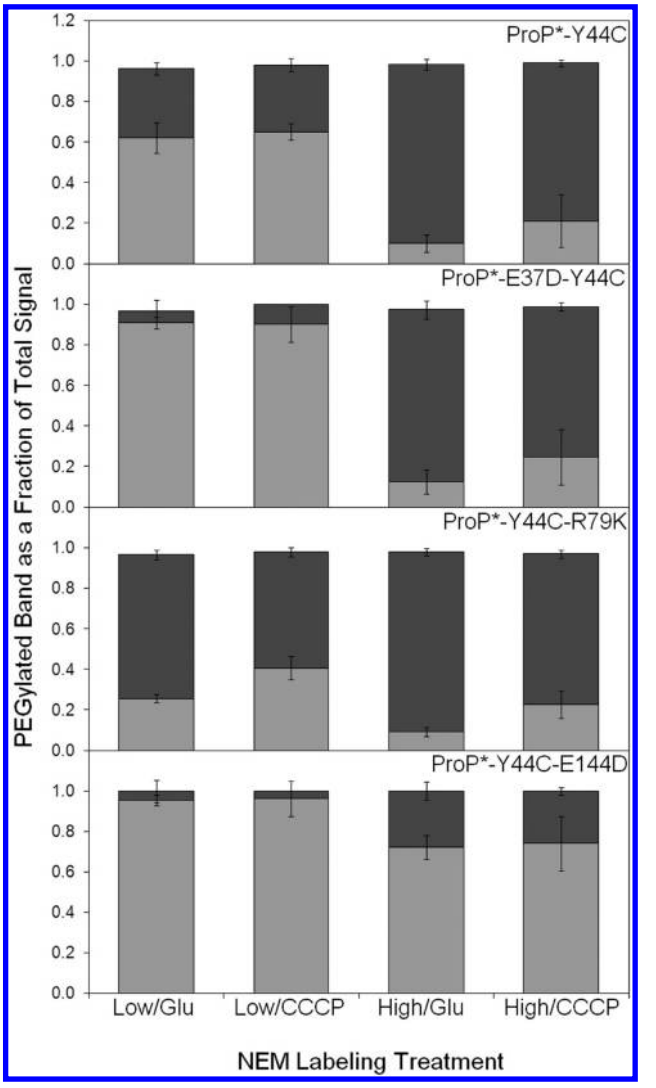

FIGURE 8: NEM reactivity of 44C depends on the osmolality. Bacteria expressing ProP*Y44C or its derivatives with additional replacement E37D, R79K, or E144D were (overlying gray bars) or were not (underlying black bars) treated with NEM (100 μM) in medium supplemented with glucose or CCCP and at low (0.15 mol/kg) or high (0.43 mol/kg) osmolality before solubilization and labeling with MalPEG, as described in the legend of Figure 4. The proportions of PEGylated and unPEGylated ProP were determined by Western blotting, as described, for three independent experiments, and error bars represent standard deviations of the means.

but are predicted to be in the cytoplasmic boundary layer of TMI and may be somewhat exposed on the cytoplasmic side. PEGylation was blocked by NEM for residues 52−65 (Figure 4). MTSEA reacted well with Cys at position 52 (Figure 3), although OGM labeled it poorly. OGM also labeled 64C and 65C poorly. Residues 52, 64, and 65 may be interfacial so that their reactivities with large anionic OGM may be limited sterically and by the electron dense environment of the carbonyl region of the ester-linked fatty acids. Anionic MTSES also did not react well with C52, whereas cationic MTSET reacted better. Overall, the data are consistent with our model (*10*). They suggest that TMI extends from approximately S31 to G52 and that V63 is near the periplasmic end of TMII.

Periplasmic Loop 1. The reactivities of Loop P1 residues provide insight into the structural dynamics of ProP even though the structure of Loop P1 remains uncertain. Our model represents a cytoplasm-facing transporter in which TMI slants into the core of ProP with the cytoplasmic end on the periphery of the TM bundle. The periplasmic loops of ProP are tightly clustered, the periplasmic end of TMI residing in the middle of the anionic, periplasmic surface of the TM bundle. In de-energized membrane fragments, residues V54, F55, and F56 were less accessible to anionic OGM and MTSES than to MTSEA, which exists as

uncharged and cationic species at neutral pH, or to uncharged NEM. The pattern of OGM labeling (Figure 2A), in which C53 and C57 are labeled but C54, C55, and C56 are not, would be consistent with the formation of a short helix embedded parallel to the membrane surface, with K53 and P57 exposed and V54, F55, and F56 buried. The presence of glycine (G52) would allow for kinking of the helix as TMI emerges from the bilayer. Thus, in the absence of $\Delta\mu_{H^+}$ at low osmolality, ProP may adopt a cytoplasm-facing conformation, in which the TM helices are tightly packed at the anionic, periplasmic membrane surface. Data reviewed below suggest that a different structure is favored at high osmolality.

Intramembrane Polar Residues Implicated in Transport Cluster in the N-Terminal Domain of ProP. Often the most conserved residues in a protein form a tight cluster in a functionally significant site (*28*, *29*). By defining the position of TMI, our data support the prediction that conserved polar and charged residues form a contiguous cluster, within hydrogen bonding distance or H_2O-bridged hydrogen bonding distance of each other, in the N-terminal helix bundle of ProP (Figure 1C). E37 and D40 are highly conserved among ProP homologues, including known α-ketoglutarate, dicarboxylate, citrate, and shikimate transporters as well as ProP orthologues. Residues Y44, R79, K134, Q137, and E144 are also conserved (Figure 1B, C). In a set of 500 such sequences descending to less than 30% overall sequence identity, the only conserved polar residues are [ED]37, [DE]40, Y44, R79, [KR]134, and Q137, within the TM region, and E144 at the cytoplasmic boundary of TMIV. The data discussed above suggest that E37 and D40 are deep in the TM region of ProP (Figure 1B,C) and their side chains face the polar cavity of the transporter molecule. These residues and others within TMI are critical for proline transport (Figures 2B,C and 5) as would be expected if they interact with H^+ and/or osmoprotectants. G33 and G42 may contribute conformational mobility, and aromatic residues (including W38, F39, F41, Y44, F46, and Y49) could interact with the quaternary ammonium groups of substrates via cation−π interactions, as observed for other transporters (*30*−*32*). However, it is important to note that the effects of the listed amino acid substitutions on transport activity could also arise from long-range effects on the three-dimensional protein structure.

The cluster of polar residues within the N-terminal helix bundle of ProP is structurally and functionally analogous to a corresponding cluster within the C-terminal domain of LacY (*17*). Recent evidence indicates that many membrane proteins are comprised of two domains, with similar folds, that are oriented in either the same orientation or opposite orientations (*33*). Such proteins may have evolved via gene duplication, fusion, and then divergence of the fused domains. Key residues in LacY are believed to participate directly in H^+ or β-galactoside transport, whereas others form intramembrane salt bridges (*17*). Residues E37, R79, and E144 of ProP may fall in the former category, whereas D40 and K134 may form a salt bridge. ProP residues E37 and D40 (in TMI) may be structurally and functionally analogous to LacY residues D237 and D240 (in TMVII). Future work will further define the roles of these residues.

Structural Mechanism of Osmosensing. We aim to understand how the osmotic pressure and the membrane potential ($\Delta\Psi$) influence the structural mechanism of H^+-osmoprotectant symport via ProP. In this study, Cys residues introduced into TMI and Loop P1 showed similar patterns of reactivity with OGM and MTS reagents in permeabilized, de-energized membranes (Figures 2A and 3, respectively) and with NEM in energized intact cells (Figure 4). Thus, at low osmolality, there is no dramatic movement of TMI normal to the membrane in response to $\Delta\mu_{H^+}$.

We also report the effects of increasing osmolality on the NEM reactivities of Cys residues at five positions lining the most polar face of TMI, both in energized cells and in the presence of CCCP (Figure 7). As previously reported for C59 (*3*), the NEM reactivities of C48, C44, and C41 increased at high osmolalities. Replacement of glucose with CCCP moderated this effect slightly but did not block it. Our functional data had suggested that osmosensing is contingent on $\Delta\Psi$. In proteoliposomes, ProP activity was osmolality-insensitive when $\Delta\Psi$ was low (0 or −100 mV); activity was suppressed at low osmolality when a $\Delta\Psi$ characteristic of respiring *E. coli* was imposed (−137 mV) (*3*). LacY activity decreases systematically as the osmolality increases over the range that elicits ProP activation. Our current data suggest that the osmolality and $\Delta\Psi$ can affect ProP independently, the net result being osmolality-independent ProP activity at intermediate $\Delta\Psi$ values. They also suggest that the (regulatory) impact of $\Delta\Psi$ on ProP structure is more subtle than the impact of the osmolality.

Like LacY, ProP is believed to follow an alternating access transport mechanism (*3*). In the absence of substrate, an equilibrium may exist between two ProP conformations: inward-facing, in which a cavity leads to the substrate binding site from the cytoplasm, and outward-facing, in which the cytoplasmic cavity is closed and a pathway to the substrate binding site from the periplasm is opened. For LacY, Kaback and his colleagues have shown that ligand addition increases the reactivities of Cys residues located on the periplasmic side of the sugar binding site whereas it decreases the reactivities of residues on the cytoplasmic side (*34*, *35*). All existing crystal structures for members of the MFS represent inward-facing conformations, so the magnitudes of these conformational changes are not known. Studies of members of the sodium symporter superfamily (*36*, *37*) and the BCCT family (including BetP) (*38*) have revealed that relatively small displacements of loops and helical components may be sufficient to expose a substrate binding site on the opposite face of the membrane, and that wholesale eversion of the transporter (the rocker switch model) may not be necessary. This work showed that the periplasm-proximal Cys residues lining the most polar face of TMI increased in NEM reactivity at high osmolality, whereas those closer to the cytoplasm did not (Figure 7). Thus, the osmolality may act by shifting equilibria between outward-facing (periplasm) and inward-facing (cytoplasm) conformations of ProP. However, the magnitude of the conformational change required to effect such reactivity changes is not yet known.

Residues in a membrane-embedded polar cluster within LacY are thought to be crucial to transitions between conformations in the transport cycle (*17*). Mutations R79K and E144D may influence the NEM reactivity of ProP*Y44C in an analogous way. The increased NEM reactivity at low osmolality of ProP*Y44C_R79K relative to ProP*Y44C (Figure 8) may reflect a bias toward an outward-facing conformation, whereas the decreased reactivity at high osmolality of ProP*Y44C_E144D may reflect a bias toward an inward-facing conformation.

Transporters ProP, BetP, and OpuA serve as paradigms for the study of osmosensing (*6*). They represent distinct transporter families, but each possesses an extended C-terminal domain implicated in osmoregulation. Analyses of osmosensing by BetP and OpuA suggest that the osmolality controls interactions of the

C-terminal domain with each transporter or membrane surface, thereby switching the transporter between inactive and active conformations. Osmolality changes may alter the structures of the membrane-embedded helix bundles of BetP and OpuA, but no evidence of such effects has been reported. The C-terminal coiled-coil domain of ProP determines its subcellular localization and adjusts the osmolality range over which transport activity varies, but it is not required for osmosensing (*39*). Data reported here suggest that, for ProP at least, the osmolality shifts the equilibria between transport pathway intermediates. Such mechanism-based osmosensing may not require the participation of an osmotic switch.

REFERENCES

1. Houssin, C., Eynard, N., Shechter, E., and Ghazi, A. (1991) Effect of osmotic pressure on membrane energy-linked functions in *Escherichia coli*. *Biochim. Biophys. Acta 1056*, 76–84.
2. Meury, J. (1994) Immediate and transient inhibition of the respiration of *Escherichia coli* under hyperosmotic shock. *FEMS Microbiol. Lett. 121*, 281–286.
3. Culham, D. E., Romantsov, T., and Wood, J. M. (2008) Roles of K^+, H^+, H_2O and $\Delta\Psi$ in solute transport mediated by Major Facilitator Superfamily members ProP and LacY. *Biochemistry 47*, 8176–8185.
4. Wood, J. M. (2010) in Bacterial Stress Responses (Storz, G., and Hengge, R., Eds.) ASM Press, Washington, DC.
5. Altendorf, K., Booth, I. R., Gralla, J. D., Greie, J.-C., Rosenthal, A. Z., Wood, J. M. (2009) EcoSal-*Escherichia coli* and *Salmonella*: Cellular and Molecular Biology (Böck, A., Curtiss, R., III, Kaper, J. B., Karp, P. D., Neidhardt, F. C., Nyström, T., Slauch, J. M., Squires, C. L., and Ussery, D., Eds.) Chapter 5.4.5, Osmotic Stress, ASM Press, Washington DC.
6. Wood, J. M. (2006) Osmosensing by bacteria. *Sci. STKE 357*, No. pe43.
7. MacMillan, S. V., Alexander, D. A., Culham, D. E., Kunte, H. J., Marshall, E. V., Rochon, D., and Wood, J. M. (1999) The ion coupling and organic substrate specificities of osmoregulatory transporter ProP in *Escherichia coli*. *Biochim. Biophys. Acta 1420*, 30–44.
8. Milner, J. L., Grothe, S., and Wood, J. M. (1988) Proline porter II is activated by a hyperosmotic shift in both whole cells and membrane vesicles of *Escherichia coli* K12. *J. Biol. Chem. 263*, 14900–14905.
9. Racher, K. I., Voegele, R. T., Marshall, E. V., Culham, D. E., Wood, J. M., Jung, H., Bacon, M., Cairns, M. T., Ferguson, S. M., Liang, W.-J., Henderson, P. J. F., White, G., and Hallett, F. R. (1999) Purification and reconstitution of an osmosensor: Transporter ProP of *Escherichia coli* senses and responds to osmotic shifts. *Biochemistry 38*, 1676–1684.
10. Wood, J. M., Culham, D. E., Hillar, A., Vernikovska, Ya. I., Liu, F., Boggs, J. M., and Keates, R. A. B. (2005) Structural model for the osmosensor, transporter, and osmoregulator ProP of *Escherichia coli*. *Biochemistry 44*, 5634–5646.
11. Culham, D. E., Vernikovska, Y. I., Tschowri, N., Keates, R. A. B., Wood, J. M., and Boggs, J. M. (2008) Periplasmic loops of osmosensory transporter ProP in *Escherichia coli* are sensitive to osmolality. *Biochemistry 47*, 13584–13593.
12. Huang, Y., Lemieux, M. J., Song, J., Auer, M., and Wang, D.-N. (2003) Structure and mechanism of the glycerol-3-phosphate transporter from *Escherichia coli*. *Science 301*, 616–620.
13. Abramson, J., Smirnova, I., Kasho, V., Verner, G., Kaback, H. R., and Iwata, S. (2003) Structure and mechanism of the lactose permease of *Escherichia coli*. *Science 301*, 610–615.
14. Yin, Y., He, X., Szewczyk, P., Nguyen, T., and Chang, G. (2006) Structure of the Multidrug Transporter EmrD from *Escherichia coli*. *Science 312*, 741–744.
15. Culham, D. E., Hillar, A., Henderson, J., Ly, A., Vernikovska, Ya. I., Racher, K. I., Boggs, J. M., and Wood, J. M. (2003) Creation of a fully functional, cysteine-less variant of osmosensor and proton-osmoprotectant symporter ProP from *Escherichia coli* and its application to assess the transporter's membrane orientation. *Biochemistry 42*, 11815–11823.
16. Liu, F., Culham, D. E., Vernikovska, Ya. I., Keates, R. A. B., Boggs, J. M., and Wood, J. M. (2007) Structure and function of the XIIth transmembrane segment in osmosensor and osmoprotectant transporter ProP of *Escherichia coli*. *Biochemistry 46*, 5647–5655.
17. Guan, L., and Kaback, H. R. (2006) Lessons from Lactose Permease. *Annu. Rev. Biophys. Biomol. Struct. 35*, 67–91.
18. Racher, K. I., Culham, D. E., and Wood, J. M. (2001) Requirements for osmosensing and osmotic activation of transporter ProP from *Escherichia coli*. *Biochemistry 40*, 7324–7333.
19. Miller, J. H. (1972) Experiments in Molecular Genetics, Cold Spring Harbor Laboratory Press, Plainview, NY.
20. Neidhardt, F. C., Bloch, P. L., and Smith, D. F. (1974) Culture medium for enterobacteria. *J. Bacteriol. 119*, 736–747.
21. Sambrook, J., and Russell, D. W. (2001) Molecular Cloning. A Laboratory Manual, Cold Spring Harbor Laboratory Press, Plainview, NY.
22. Kempf, B., and Bremer, E. (1998) Uptake and synthesis of compatible solutes as microbial stress responses to high osmolality environments. *Arch. Microbiol. 170*, 319–330.
23. Guzman, L.-M., Belin, D., Carson, M. J., and Beckwith, J. (1995) Tight regulation, modulation, and high-level expression by vectors containing the arabinose P_{BAD} promoter. *J. Bacteriol. 177*, 4121–4130.
24. Culham, D. E., Lasby, B., Marangoni, A. G., Milner, J. L., Steer, B. A., van Nues, R. W., and Wood, J. M. (1993) Isolation and sequencing of *Escherichia coli* gene *proP* reveals unusual structural features of the osmoregulatory proline/betaine transporter, ProP. *J. Mol. Biol. 229*, 268–276.
25. Culham, D. E., Tripet, B., Racher, K. I., Voegele, R. T., Hodges, R. S., and Wood, J. M. (2000) The role of the carboxyl terminal α-helical coiled-coil domain in osmosensing by transporter ProP of *Escherichia coli*. *J. Mol. Recognit. 13*, 1–14.
26. Culham, D. E., Henderson, J., Crane, R. A., and Wood, J. M. (2003) Osmosensor ProP of *Escherichia coli* responds to the concentration, chemistry and molecular size of osmolytes in the proteoliposome lumen. *Biochemistry 42*, 410–420.
27. Lu, J., and Deutsch, C. (2001) Pegylation: A method for assessing topological accessibilities in Kv1.3. *Biochemistry 40*, 13288–13301.
28. Yao, H., Kristensen, D. M., Mihalek, I., Sowa, M. E., Shaw, C., Kimmel, M., Kavraki, L., and Lichtarge, O. (2003) An accurate, sensitive, and scalable method to identify functional sites in protein structures. *J. Mol. Biol. 326*, 255–261.
29. Lee, D., Redfern, O., and Orengo, C. (2007) Predicting protein function from sequence and structure. *Nat. Rev. Mol. Cell Biol. 8*, 995–1005.
30. Smits, S. H., Höing, M., Lecher, J., Jebbar, M., Schmitt, L., and Bremer, E. (2008) The compatible-solute-binding protein OpuAC from *Bacillus subtilis*: Ligand binding, site-directed mutagenesis, and crystallographic studies. *J. Bacteriol. 190*, 5663–5671.
31. Sohn-Basser, L., Hanekop, N., Höing, M., Sohn-Bösser, L., Jebbar, M., Schmitt, L., and Bremer, E. (2007) Crystal structure of the ligand-binding protein EhuB from *Sinorhizobium meliloti* reveals substrate recognition of the compatible solutes ectoine and hydroxyectoine. *J. Mol. Biol. 374*, 1237–1250.
32. Horn, C., Sohn-Bösser, L., Breed, J., Welte, W., Schmitt, L., and Bremer, E. (2006) Molecular determinants for substrate specificity of the ligand-binding protein OpuAC from *Bacillus subtilis* for the compatible solutes glycine betaine and proline betaine. *J. Mol. Biol. 357*, 592–606.
33. Sobczak, I., and Lolkema, J. S. (2005) Structural and mechanistic diversity of secondary transporters. *Curr. Opin. Microbiol. 8*, 161–167.
34. Kaback, H. R., Dunten, R., Frillingos, S., Venkatesan, P., Kwaw, I., Zhang, W., and Ermolova, N. (2007) Site-directed alkylation and the alternating access model for LacY. *Proc. Natl. Acad. Sci. U.S.A. 104*, 491–494.
35. Ermolova, N., Madhvani, R. V., and Kaback, H. R. (2006) Site-directed alkylation of cysteine replacements in the lactose permease of *Escherichia coli:* Helices I, III, VI, and XI. *Biochemistry 45*, 4182–4189.
36. Singh, S. K., Piscitelli, C. L., Yamashita, A., and Gouaux, E. (2008) A competitive inhibitor traps LeuT in an open-to-out conformation. *Science 322*, 1655–1661.
37. Shimamura, T., Weyand, S., Beckstein, O., Rutherford, N. G., Hadden, J. M., Sharples, D., Sansom, M. S., Iwata, S., Henderson, P. J., and Cameron, A. D. (2010) Molecular basis of alternating access membrane transport by the sodium-hydantoin transporter Mhp1. *Science 328*, 470–473.
38. Ressl, S., Terwisscha van Scheltinga, A. C., Vonrhein, C., Ott, V., and Ziegler, C. (2009) Molecular basis of transport and regulation in the Na^+/betaine symporter BetP. *Nature 458*, 47–52.
39. Romantsov, T., and Wood, J. M. (2009) Cardiolipin and the osmotic stress responses of bacteria. *Biochim. Biophys. Acta 1788*, 2092–2100.